[5] K. Tomiyasu, "Short pulse wide-band Scatterometer ocean surface signature," *IEEE Trans. Geosci. Electron. (Special Issue on Remote Sensing)*, vol. GE-9, pp. 175–177, July 1971.
[6] J. Eckerman, "Satellite instrumentation for ocean surface measurements," presented at the 1974 IEEE INTERCON, New York, Mar. 26–29, 1974.
[7] N. W. Guinard and J. C. Daley, "An experimental study of sea clutter model," *Proc. IEEE*, vol. 58, pp. 543–550, Apr. 1970.
[8] G. R. Valenzuela, M. B. Laing, and J. C. Daley, "Ocean spectra for the high frequency waves as determined from airborne radar measurements," *J. Marine Res.*, vol. 29, no. 2, 1971.
[9] J. C. Daley, "An empirical sea clutter model," NRL Memo Rep. 2668, Dec. 1973.
[10] K. Krishen, "Correlation of radar backscattering cross sections with ocean wave height and wind velocity," Lockheed Electronics Co., Houston, Tex., TR 649D. 21.025, March 1970.
[11] G. A. Bradley, "Remote sensing of ocean winds using a radar scatterometer," Ph.D. dissertation, Univ. Kansas Center for Research, Inc., 1971.
[12] J. P. Claassen and H. S. Fung, "The wind response of radar sea return and its implication on wave spectral growth," Univ. Kansas Center for Research, Inc., Tech. Rep. 186-5, Sept. 1971.
[13] J. R. Apel, "A hard look at oceans from space," presented at the AIAA 9th Annu. Meeting, Washington, D. C., Jan. 8–10, 1973, Paper no. 73-11.
[14] C. T. Swift and W. L. Jones, "Satellite radar scatterometry," presented at the 1974 IEEE INTERCON, New York, Mar. 26–29, 1974.
[15] W. L. Jones, W. L. Grantham, L. C. Schroeder, and J. L. Mitchell, "Microwave scatterometer measurements of ocean wind vector," presented at the 1974 USNC/URSI Meeting, Boulder, Colo., Oct. 1974.
[16] V. J. Cardone, "Specification of the wind distribution in the marine boundary layer for wave forecasting," New York Univ., School of Engineering and Science, New York, Mar. 1970, Rep. TR69-1 (available as DDS no. AD702 490).
[17] R. K. Moore *et al.*, "Simultaneous active and passive microwave response of the earth—The Skylab RADSCAT experiment," in *Proc. 9th Symp. Remote Sensing of the Environment* (Ann Arbor, Mich., April 1974).
[18] D. Ross *et al.*, "Remote sensing of pacific hurricane and radiometric measurements from foam and slicks," NOAA, Miami, Fla., Progress Rep. NASA CR 140126, July 31, 1974.
[19] A. K. Jordan, C. G. Purves, and J. F. Diggs, "Analyses of Skylab II S-193 scatterometer data," NRL Rep. 7877, May 2, 1975.
[20] W. L. Grantham *et al.*, "An operational satellite scatterometer for wind vector measurements over the ocean," NASA TM-X 72672, Mar. 1975.

Microwave Irradiation Design Using Dielectric Lenses

HENRY S. HO, MEMBER, IEEE, GARY J. HAGAN, AND MARK R. FOSTER

***Abstract*—Theoretical calculations and electric-field measurements were made to investigate the focusing effects of plane-wave-irradiated dielectric spheres (lenses). Spheres of different diameters and dielectric properties and plane wave sources of different frequencies were used in the calculations. The results indicate the feasibility of using dielectric lenses for selective partial-body irradiation in biological experiments.**

INTRODUCTION

The use of concentrated microwave beams for communication between distant stations has been widely investigated, resulting in dramatic advances in modern antenna and radar designs. However, in the area of biological researches and medical applications of microwaves, it may be desirable to focus microwave energy in a very small region in the proximity of the focusing lens. One application of this technique involves the selective heating of rabbit eyes with a dielectric lens for microwave cataractogenesis experiments [1].

In the current investigation, theoretical calculations and electric-field measurements are made to determine the focused effects of electric fields behind a plane-wave-irradiated dielectric sphere (lens) [2], [3]. Parameters for this investigation include sizes and dielectric properties of the sphere and the frequency of the incident plane wave.

CALCULATIONS OF ELECTROMAGNETIC FIELDS BEHIND A PLANE-WAVE-IRRADIATED DIELECTRIC SPHERE

The formulation for the scattered electromagnetic fields from a plane-wave-irradiated dielectric sphere has been reported by Stratton [4]. The total field at a location is therefore the summation of the incident plane-wave field and the scattered field at that location. Based on this formulation, a computer program is written to calculate the electric field patterns behind a plane-wave-irradiated dielectric sphere. The direction of the electric field behind the dielectric sphere is also determined. Fig. 1 shows a plane-wave-irradiated dielectric sphere with a set of rectangular coordinates. An X–Y plane is shown behind the dielectric sphere. The electric fields squared on X–Y, X–Z, and Y–Z planes are calculated and presented in "three-dimensional" plots. The electric fields squared on all the planes are normalized to the incident plane-wave electric field squared. The magnitude of the peak of the normalized electric-field-squared pattern on each X–Y plane is defined as the focusing factor on the plane. The focusing factor of each X–Y plane depends on the distance of the plane behind the dielectric sphere. Eight different sphere sizes, three different dielectric materials, and two source frequencies are used for the calculation. The sphere diameters range from 5.1 cm through 40.6 cm. The dielectric materials are polyethylene ($\epsilon' = 2.26$, $\tan\delta = 3.6 \times 10^{-4}$), polyfoam ($\epsilon' = 1.98$, $\tan\delta = 7.0 \times 10^{-4}$), and Emerson and Cumings, Inc. Stycast 35 DA ($\epsilon' = 5.0$, $\tan\delta = 10 \times 10^{-4}$). The source frequencies are 2450 MHz and 10 GHz.

RESULTS OF THEORETICAL CALCULATIONS

Fig. 2(a) shows the normalized electric-field-squared pattern in a 40-cm × 40-cm X–Y plane at the location of maximum focusing behind a 20.3-cm-diam polyfoam sphere which is irradiated by a 2450-MHz plane wave. The plane is located directly behind the sphere at $d = 0$ cm because the focal point is inside the sphere. The patterns of the normalized electric field squared on 40-cm × 20-cm X–Z and Y–Z planes for the same 20.3-cm-diam polyfoam sphere and 2450-MHz incident plane wave are shown in Fig. 2(b), (c). These patterns show a gradual decrease of the peak of the focused

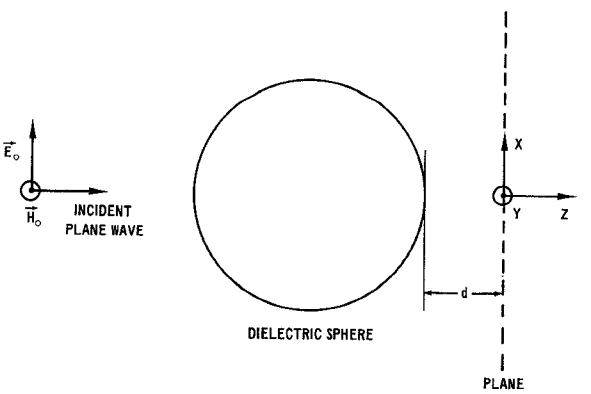

Fig. 1. An X–Y plane behind a dielectric sphere irradiation by an electromagnetic plane wave. Characters with arrows in figure appear as boldface italic in text.

Manuscript received April 18, 1975; revised August 15, 1975.
The authors are with the Division of Biological Effects, Bureau of Radiological Health, Food and Drug Administration, Public Health Service, U. S. Department of Health, Education, and Welfare, Rockville, Md. 20852.

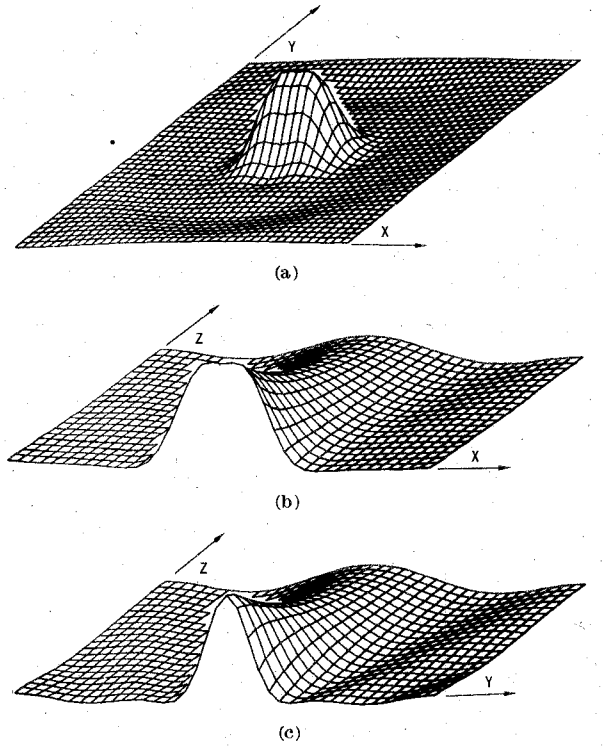

Fig. 2. (a) Normalized electric field squared in an X–Y plane at the location of maximum focusing behind a 20.3-cm-diam polyfoam sphere. Dimensions: $-20 \leq X \leq 20$ cm, $-20 \leq Y \leq 20$ cm, $d = 0$ cm. Frequency = 2450 MHz. Peak = 13.9. (b) Normalized electric field squared in an X–Z plane behind a 20.3-cm-diam polyfoam sphere. Dimensions: $-20 \leq X \leq 20$ cm, $Y = 0$ cm, $0 \leq d \leq 20$ cm. Frequency = 2450 MHz. Peak = 13.9. (c) Normalized electric field squared in an Y–Z plane behind a 20.3-cm-diam polyfoam sphere. Dimensions: $X = 0$ cm, $-20 \leq Y \leq 20$ cm, $0 \leq d \leq 20$ cm. Frequency = 2450 MHz. Peak = 13.7.

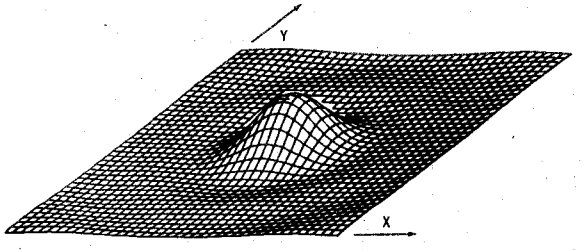

Fig. 3. Normalized electric field squared in an X–Y plane behind a 20.3-cm-diam polyfoam sphere. Dimensions: $-20 \leq X \leq 20$ cm, $-20 \leq Y \leq 20$ cm, $d = 6$ cm. Frequency = 2450 MHz. Peak = 8.5

beam along the Z direction in contrast to its sharply focused shape along the X and Y directions. Fig. 3 shows the normalized electric field squared in a 40-cm × 40-cm X–Y plane at $d = 6$ cm behind the sphere. The beam of the focused electric field has an elliptic cross section with the long side parallel to the direction of the electric field of the incident plane wave (E_0). The peak of the focused beam at 6 cm behind the sphere (8.5) is reduced from that at maximum focusing (13.9). Table I summarizes the maximum focusing factor and the focusing factor at 6 cm behind the 2450-MHz-plane-wave-irradiated dielectric spheres of three different materials and eight different sizes. It is found that the focusing factors for the 40.6-cm-diam sphere are much higher than those for the 5.1-cm diameter. However, it should be noted that the focusing factors do not always increase with increasing sphere diameter. In fact the focusing factor for the Emerson and Cumings Stycast 35 DA sphere fluctuates as the diameter increases beyond 15.2 cm. The data also indicate that the focusing factor decreases with distance behind the sphere in different amounts for the three different dielectric materials. For example, at

TABLE I
FOCUSING FACTOR BEHIND A DIELECTRIC SPHERE FOR AN INCIDENT 2450-MHz PLANE WAVE

Sphere Diameter (cm)	POLYETHYLENE $\varepsilon'=2.26$, $\tan\delta=3.6\times10^{-4}$			POLYFOAM $\varepsilon'=1.89$, $\tan\delta=7.0\times10^{-4}$			E. & C. STYCAST 35 DA $\varepsilon'=5.0$, $\tan\delta=10\times10^{-4}$		
	f_m	d_m (cm)	f_a	f_m	d_m (cm)	f_a	f_m	d_m (cm)	f_a
5.1	1.5	1.6	1.3	1.4	1.8	1.3	4.8	0.0*	1.8
10.2	5.2	0.0*	3.0	3.6	0.4*	2.6	8.2	0.0*	0.06
15.2	10.7	0.0*	4.7	8.0	0.0*	5.1	25.9	0.0*	1.2
20.3	19.2	0.0*	6.7	13.9	0.0*	8.5	13.6	0.0*	1.8
25.4	35.1	0.0*	9.6	19.8	0.0*	12.3	12.9	0.0*	1.0
30.5	34.4	0.0*	9.3	29.5	0.0*	18.3	7.6	0.0*	3.5
35.6	49.7	0.0*	14.3	28.8	1.2	21.0	17.2	0.0*	2.0
40.6	54.5	0.0*	22.7	37.6	2.0	30.2	20.8	0.0*	4.8

Note: f_m is the maximum focusing factor behind the dielectric sphere.
d_m is the distance behind the sphere where maximum focusing occurs.
* indicates that the focal point is inside the sphere.
f_a is the focusing factor at 6 cm behind the sphere.

6 cm behind the Stycast 35 DA sphere, the focusing effect is virtually lost, whereas at the same distance the polyethylene and polyfoam spheres retain focusing effects.

Fig. 4(a) shows the normalized electric-field-squared pattern in a 40-cm × 40-cm X–Y plane at the location of maximum focusing behind a 10-GHz-plane-wave-irradiated 20.3-cm-diam polyfoam sphere. Note that due to the higher peaks of the focused beams for the 10-GHz radiation, the scale of the normalized electric field squared is reduced to one-half of that of the 2450-MHz case. The beamwidth for the 10-GHz radiation is also much smaller than the beamwidth for the 2450-MHz radiation. The beamwidth of the focused radiation is defined by the maximum width across the region where the focused radiation has decreased to the value of the incident electric field. Fig. 4(b), (c) shows the field patterns in the X–Z and Y–Z planes behind the 20.3-cm-diam polyfoam sphere. Again the peak of the focused beam rises to a maximum at the focal point behind the sphere and attenuates faster than that of the 2450-MHz case. Note also the severe splitting of the beam (double peaks) close to the surface of the dielectric sphere. Table II summarizes the maximum focusing factor and the focusing factor at 6 cm behind 10-GHz-plane-wave-irradiated spheres of three different materials and eight different sizes. The general behavior of the focused radiation for 10 GHz closely resembles that of 2450 MHz. However, the 10-GHz case has higher focusing factors and also more of the spheres have focal points outside the sphere.

The amplitude and phase of the focused electric field are computed and expressed as components along the X, Y, and Z directions. It is found that whereas the incident electric field is linearly polarized along the X direction, the focused electric field, in general, possesses all X, Y, and Z components. The phase of the electric field also changes with position. However, along the X–Z plane with $Y = 0$ cm, the electric field has only in-phase X and Z components and is therefore linearly polarized. Along the Y–Z plane with $X = 0$ cm, the electric field has an X component only and is therefore also linearly polarized.

MEASUREMENT OF AN ELECTRIC FIELD BEHIND A DIELECTRIC SPHERE

Electric field measurements are made in an anechoic chamber behind a 20.3-cm-diam polyfoam sphere irradiated by 2450-MHz CW microwave radiation from a standard gain horn located 150 cm

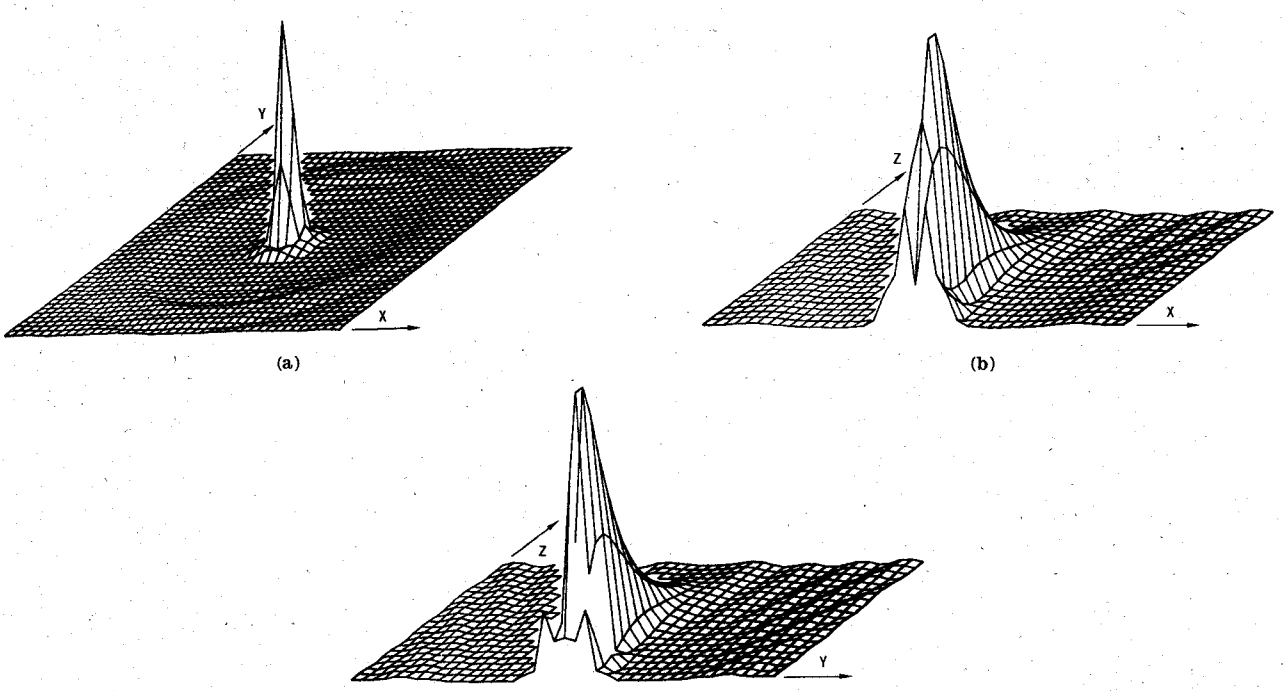

Fig. 4. (a) Normalized electric field squared in an X–Y plane at the location of maximum focusing behind a 20.3-cm-diam polyfoam sphere. Dimensions: $-20 \leq X \leq 20$, $-20 \leq Y \leq 20$ cm, $d = 2.4$ cm. Frequency = 10 GHz. Peak = 71.8. (b) Normalized electric field squared in an X–Z plane behind a 20.3-cm-diam polyfoam sphere. Dimensions: $-20 \leq X \leq 20$ cm, $Y = 0$ cm, $0 \leq d \leq 20$ cm. Frequency = 10 GHZ. Peak = 71.8. (c) Normalized electric field squared in an Y–Z plane behind a 20.3-cm-diam polyfoam sphere. Dimensions: $X = 0$ cm, $-20 \leq Y \leq 20$ cm, $0 \leq d \leq 20$ cm, Frequency = 10 GHz. Peak = 71.8.

TABLE II
FOCUSING FACTOR BEHIND A DIELECTRIC SPHERE FOR AN INCIDENT 10-GHz PLANE WAVE

Sphere Diameter (cm)	POLYETHYLENE $\epsilon'=2.26$, $\tan\delta=3.6\times10^{-4}$			POLYFOAM $\epsilon'=1.89$, $\tan\delta=7.0\times10^{-4}$			E. & C. STYCAST 35 DA $\epsilon'=5.0$, $\tan\delta=10\times10^{-4}$		
	f_m	d_m (cm)	f_a	f_m	d_m (cm)	f_a	f_m	d_m (cm)	f_a
5.1	18.0	0.0*	1.2	14.8	0.0*	3.1	10.4	0.0*	0.2
10.2	52.9	0.0*	3.2	33.5	0.6	3.1	23.5	0.0*	0.8
15.2	70.0	0.6	6.3	66.5	1.2	12.7	28.5	0.0*	1.1
20.3	109.3	0.6	16.5	71.8	2.4	40.1	23.5	0.0*	0.3
25.4	143.5	1.6	37.7	104.2	3.6	72.2	29.0	0.0*	0.6
30.5	164.9	2.2	65.8	117.3	4.4	103.4	43.6	0.0*	1.5
35.6	205.2	2.8	103.5	147.6	6.0	147.6	36.1	0.0*	2.2
40.6	229.6	3.2	156.5	183.9	7.0	172.7	36.7	0.0*	4.1

Note: f_m is the maximum focusing factor behind the dielectric sphere.
d_m is the distance behind the sphere where maximum focusing occurs.
* indicates that the focal point is inside the sphere.
f_a is the focusing factor at 6 cm behind the sphere.

from the sphere. A Narda model 8305 radiation monitor with a model 8323 three-dimensional probe is used for the measurement. Fig. 5 shows the dielectric lens and the radiation monitor. The attachment on the dielectric lens along with a light source (not shown on the figure) are used for the alignment of the radiation monitor to desired locations behind the dielectric lens. The attachment is removed before each measurement. The measuring antenna has a 5-cm diameter. It is therefore expected that resolution of sharp peaks in field patterns is not possible with the given instrumentation. Fig. 6 shows the comparison between calculated and measured value of the normalized electric field squared in a 20-cm × 20-cm X–Y plane, 6 cm behind the polyfoam sphere. The measured and calculated results agree very well, considering the limitation of the measuring antenna. The beam is wider along the direction of incident electric field in

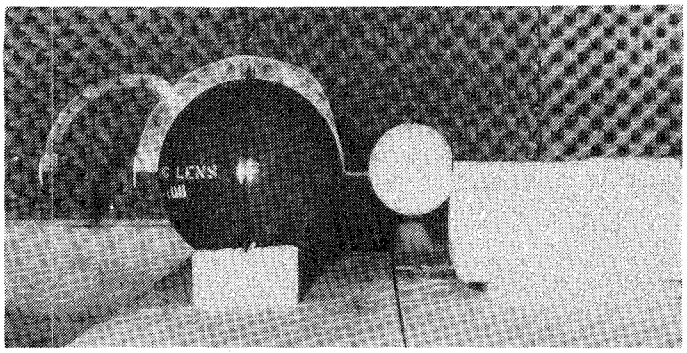

Fig. 5. Apparatus for electric field measurement behind a dielectric lens.

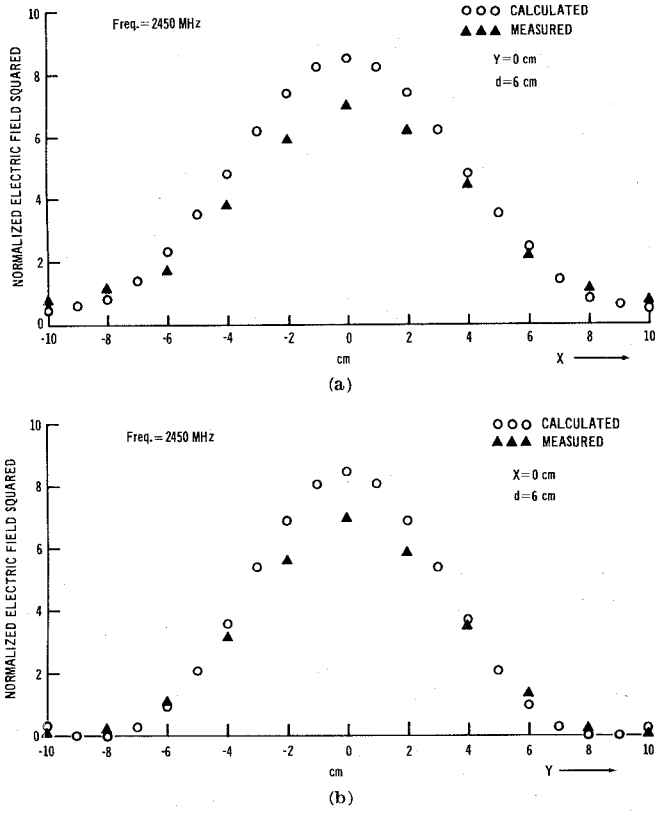

Fig. 6. Comparison of calculated and measured normalized electric field squared in a 20-cm × 20-cm X–Y plane, 6 cm behind a polyfoam sphere. (a) Along the direction of incident electric field vector (E_0). (b) Along the direction of incident magnetic-field vector (H_0).

comparison to that of incident magnetic field direction as is predicted by the calculation. The slightly lower measured peak compared to the calculated value is expected from the averaging effect of the measuring antenna which has a 5-cm diameter.

DISCUSSION

The results of the investigation indicate that the focusing effect of dielectric spheres depends on dielectric material, sphere size, and source frequency. The Stycast 35 DA dielectric material which has a relative dielectric constant of 5.0 does not perform as well as polyethylene ($\epsilon' = 2.26$) and polyfoam ($\epsilon' = 1.89$) in focusing electric fields. Hence the approach of increasing the dielectric constant in hope of increasing focusing of radiation may not be valid. The electric field may be focused internally in the sphere with $\epsilon' = 5.0$. The increase of focusing factor with increased sphere diameter is found. However, the increase is not monotonic. The source frequency affects both beamwidth of focused radiation and its peak. The result indicates that the source frequency is the primary controlling factor of the width of the base of the focused beam. However, for a highly focused beam, the value of the electric field squared at the base of the beam will be very small compared to that of the peak. For the practical applications of selective exposure, one may define a beam spot to be the region across which the focused electric field squared attenuates from its peak value to a given fraction of the peak value, such as one-tenth. The beam spot is therefore dependent on the focusing factor as well as the source frequency. Hence, the peak and the beam spot of the focused beam can be partially controlled by the magnitude of incident power density and the sphere diameter without changing source frequency.

CONCLUSION

This investigation indicates that by proper selection of source frequency, dielectric materials, and the size of the dielectric spheres, specified focused microwave radiation can be produced for localized exposure of biological subjects. This technique may also be useful for medical applications such as noncontact selective heating of diseased tissues as an alternative to surgical removal, the therapeutic selective heating of wounded tissues, and selective heating in conjunction with chemotherapy.

It should be emphasized that the electric fields calculated and measured in this investigation are exposure fields in the absence of the subject to be irradiated. It is expected that the presence of the irradiated object near this exposure field will significantly alter the exposure field. Also, the tissue penetration characteristics of such a focused microwave exposure field is as yet not determined. The significant dependence of microwave absorption patterns in tissues due to different sources (exposure fields) has been reported [5]. Additional work is needed to determine the tissue absorption characteristics of the focused exposure field. In the current investigation, the apparatus for producing a focused exposure field requires a plane-wave source and hence an anechoic chamber as well as a high-power generator. To increase the practical utility of the dielectric sphere, research may be needed to determine the possibility of replacing the incident plane-wave source with a more practical source.

REFERENCES

[1] R. L. Carpenter, E. S. Ferri, and G. J. Hagan, "Use of a dielectric lens for experimental microwave irradiation of the eye," presented at the 1974 Conf. Biological Effects of Non-ionizing Radiation, Academy of Sciences, New York, Feb. 12–15, 1974.
[2] T. C. Chestan and E. I. Luma "Constant-K lenses," in *ALP Tech. Dig.*, Mar.–Apr. 1963.
[3] G. Bekefi and G. W. Farnell, "A homogeneous dielectric sphere as a microwave lens," *Can. J. Phys.*, vol. 34, pp. 790–803, 1956.
[4] J. A. Stratton, *Electromagnetic Theory*. New York: McGraw-Hill, 1941, pp. 563–570.
[5] H. S. Ho, "Contrast of dose distribution in phantom heads due to aperture and plane wave sources," *Ann. N. Y. Acad. Sci.*, vol. 247, pp. 454–472, 1975.

On the Synthesis of Waveguides and Cavities Realized with Nonseparable Solutions of Helmholtz Wave Equation

P. J. LUYPAERT AND D. H. SCHOONAERT

***Abstract*—This short paper shows how nonseparable solutions of the Helmholtz wave equation can be used in the synthesis of waveguides and cavities with nonconventional cross section, and also investigates the attenuation and Q factor.**

Manuscript received March 17, 1975; revised July 21, 1975.
The authors are with the Department of Electronics, Catholic University of Louvain, Heverleer, Louvain, Belgium.